



Perspectives for future X-ray FELs

Claudio Pellegrini

UCLA Department of Physics and Astronomy

SLAC National Accelerator Laboratory



Why x-ray lasers?



UCLA

A laser generating high intensity, coherent X-ray pulses at Ångstrom wavelength and femtosecond pulse duration -the characteristics time and space scale for atomic and molecular phenomena- allows imaging of periodic and non periodic systems, non crystalline states, studies of dynamical processes in systems far from equilibrium, nonlinear science, **opening a new window on atomic and molecular phenomena of interest to biology, chemistry and physics.**



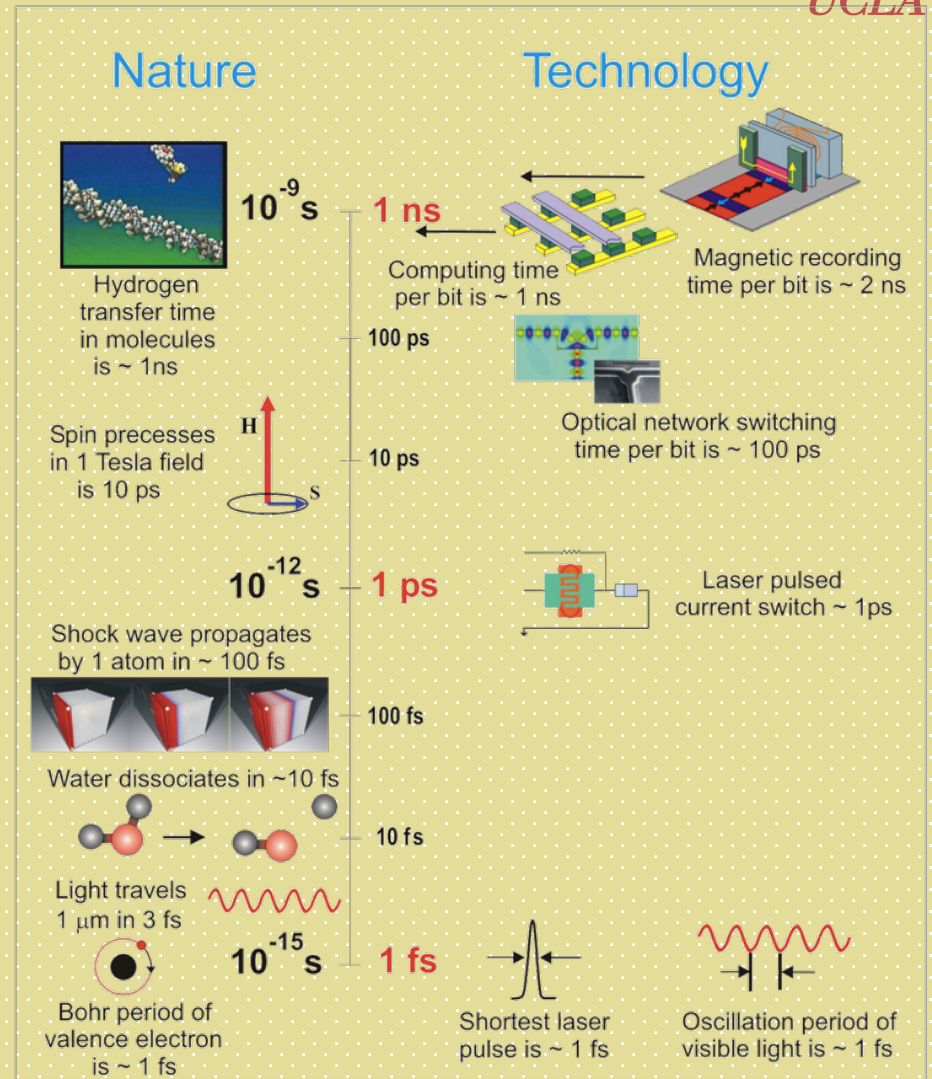
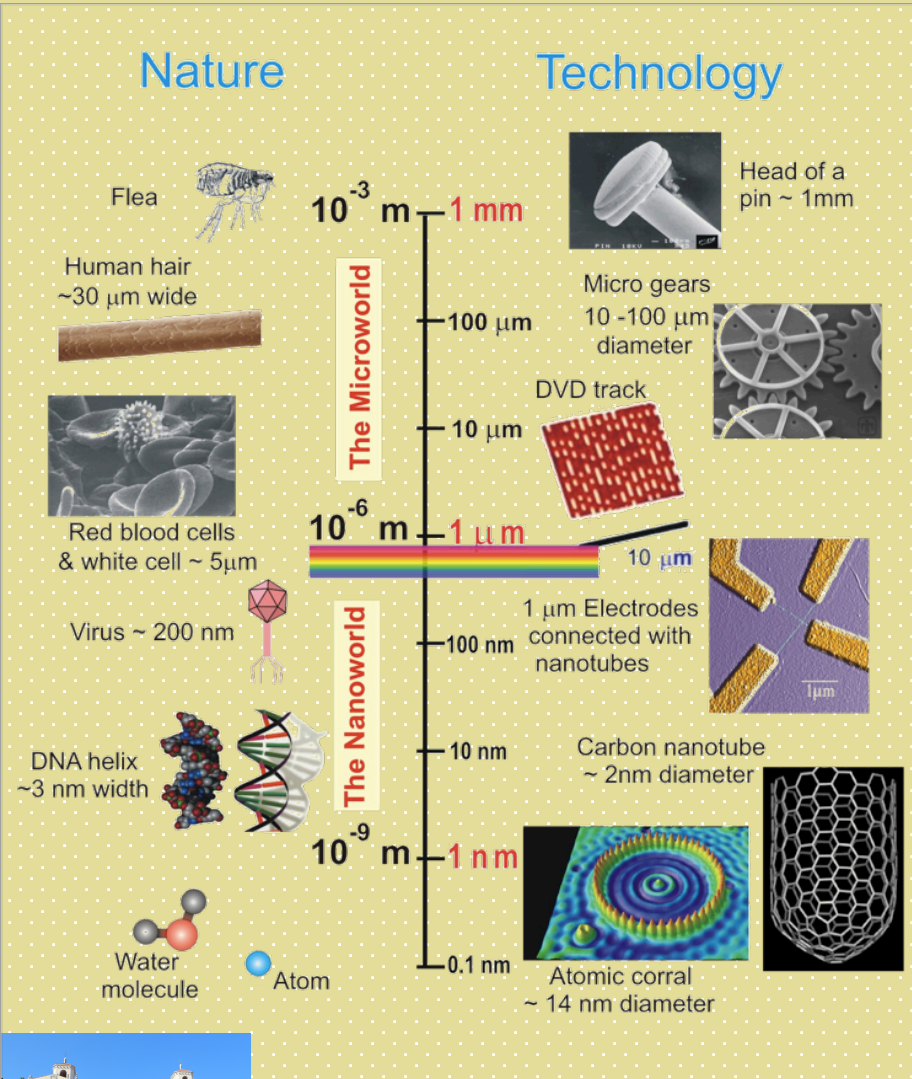
X-Rays have opened the Ultra-Small World X-FELs open the Ultra-Small and Ultra-Fast Worlds



UCLA

Ultra-Small

Ultra-Fast



Early work on X-ray lasers



UCLA

In the conventional atom-based laser approach reaching the X-ray wavelength is extremely difficult, because of the very short lifetime of excited atom-core quantum energy levels. George Chapline and Lowell Wood of the Lawrence Livermore National Laboratory estimated the radiative lifetime of an X-ray laser transition would be about 1 fs times the square of the wavelength in angstroms.

Chapline G. and L. Wood, 1975, Physics Today 40, 8.

Together with the large energy needed to excite inner atomic levels, 1 to 10 KeV compared to about 1 eV for visible lasers, this leads to a requirement for very intense pumping levels to attain population inversion, too large for practical purposes.

Building low loss optical cavities for X-ray laser oscillators is also difficult, in fact beyond the present state of the art.

But not to be discouraged: Scientists at LLNL proposed to use a nuclear weapon to drive an X-ray laser. They tried this concept in the Dauphin experiment, apparently with success, in 1980.

Hecht J., 2008, The History of the X-ray Laser, Optics and Photonics News, 19 (2008)

Early work on X-ray lasers



UCLA

The development of high peak power, short pulse, visible light lasers made possible another approach: pumping cylindrical plasmas, in some cases also confining the plasma with magnetic fields. These experiments led to X-ray lasing around 18 nm with gain of about 100 in 1985 (Matthews *et al.*, 1985; Suckewer *et al.*, 1985). More work has been done from that time and lasing has been demonstrated at several wavelengths in the soft X-ray region, however with limited peak power and tunability. A review of the most recent work and developments with this approach is given in (Suckewer and Jaeglé, 2009)

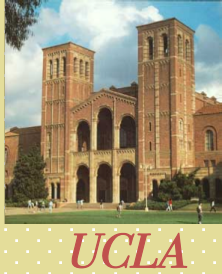
Matthews D.L. et al., 1985, Physics Review Letters **54**, 110.

Suckewer S. et al., 1985, Physics Review Letters **55**, 1753.

Suckewer S. and P. Jaeglé, 2009, Laser Physics Letters **1**, 411 (2009).



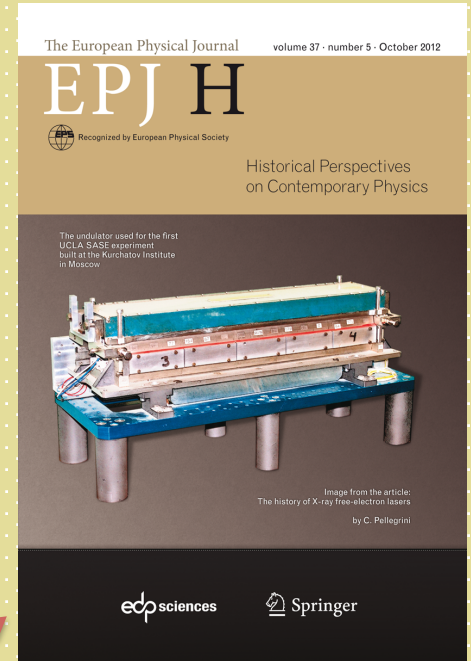
An alternative solution



The way out of this difficult situation is given by the generation of X-rays from high brightness relativistic electron beams and the FEL.

A proposal in 1992 (*C. Pellegrini, 1992 Proc. of the Workshop on 4th generation light sources, SSRL/SLAC Rep. 92/02*) to build an X-ray FEL using 1 km of the SLAC linac producing a 15GeV high brightness beam lead to the design and construction of LCLS at SLAC. In 2009 LCLS successfully started to work (*P. Emma et al., 2010 Nat. Phot. 4, 641*) with characteristics similar or better than those in the original proposal.

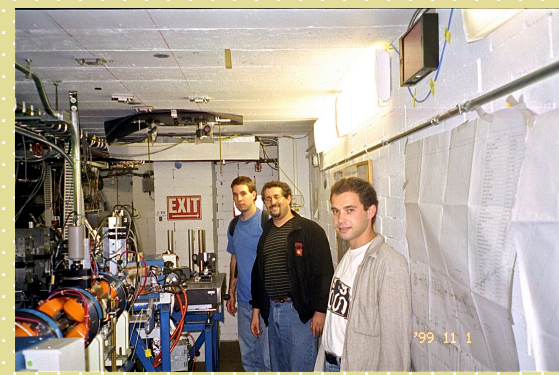
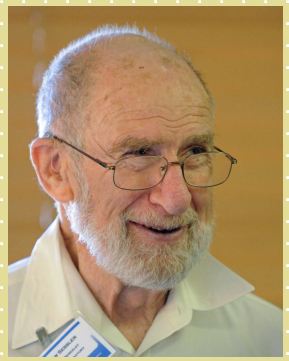
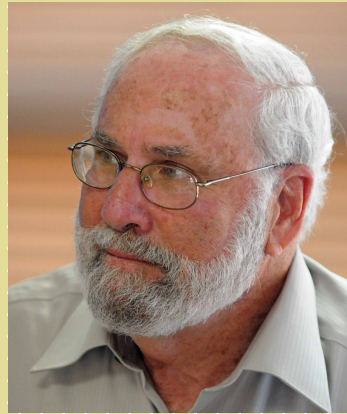
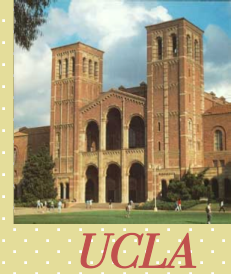
A history of this development is found in *Pellegrini, C., 2012, History of the X-ray free-electron laser, European Physics Journal H 37, 659.*



60 cm long undulator used for the first UCLA SASE FEL at 16 μm .
 Period 1.5 cm, $K=1$, gap 5mm.
Varfolomeev, A.A. et al., 1992 Nucl. Instr. and Meth. A 318, 813.



It takes a village to raise a child



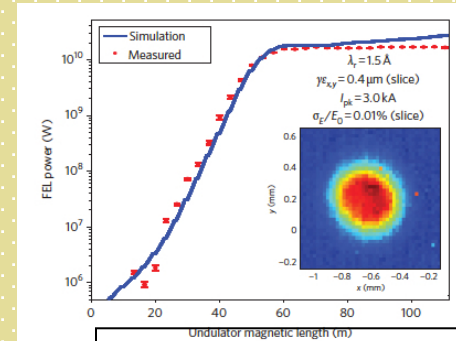
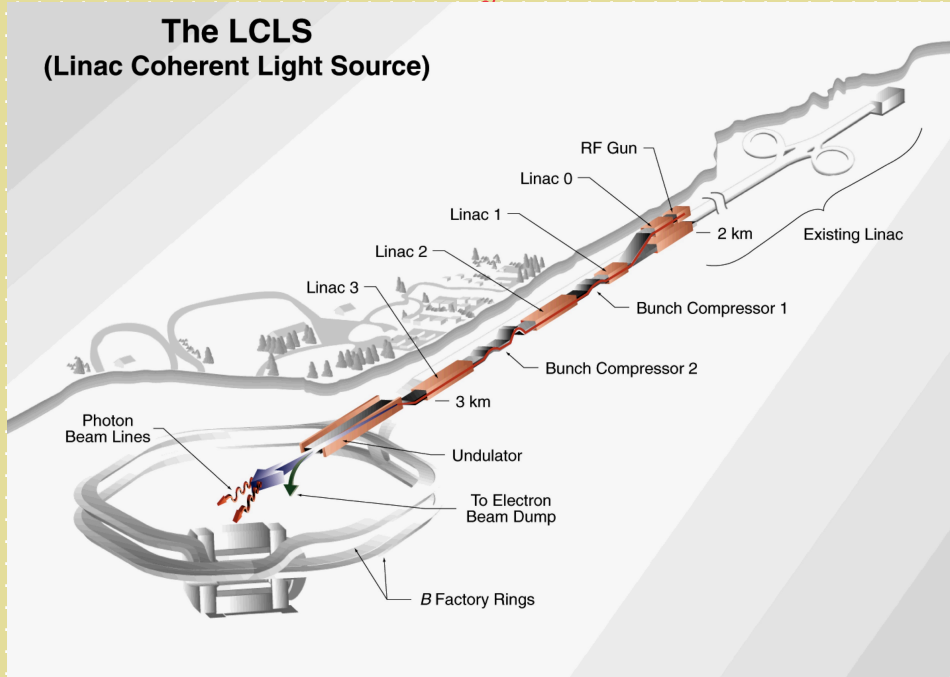
And many more



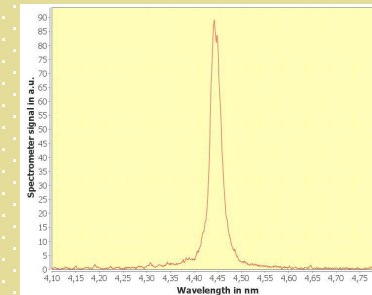
X-ray Free-electron Lasers today



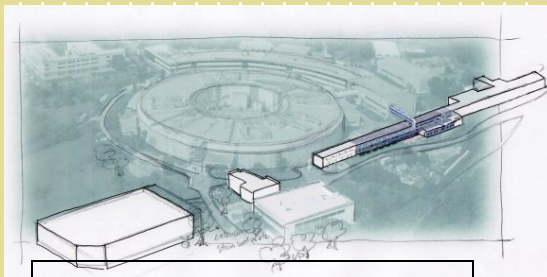
UCLA



LCLS, 1.5 Å,
4/2009, 1-3 mJ



Flash: 4.45
nm, 0.3 mJ,
6/2010



Fermi@Elettra,
43nm, 12/2010



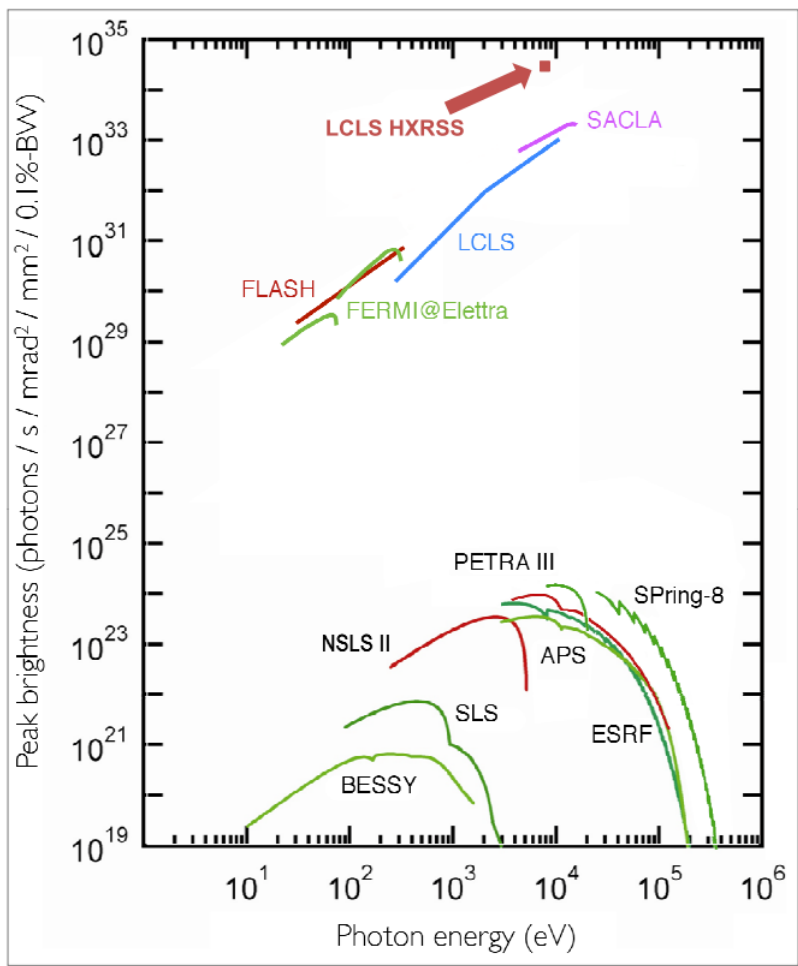
SACLA, 0.8 Å, 6/2011

New projects: European XFEL, LCLS-II, Swiss X-FEL, Korean X-FEL, Shanghai





Comparison of X-ray sources



The best quantity to compare X-ray sources is the brightness, the number of photons in the X-ray beam six dimensional phase space. In practical units it is given by number of photons/sec/mm²mrad²/0.1% bandwidth. The plot shows the peak brightness for the most advanced X-ray sources, X-ray FELs and storage rings. Notice the jump by a factor 10⁹ when LCLS started to operate in 2009.

Ref. Fletcher, L. B., et al., 2015, Nature Photonics **9**, 274.





Main X-ray FELs characteristics

Location	Name	Linac type	E energy (GeV)	Photon energy (keV)	Rep. rate (Hz)	Start ops.
Germany	FLASH	SC	1.2	0.03–0.3	$(1 - 500) \times 10^a$	2005
	FLASH-II	SC				2015
	XFEL	SC	17.5	3–25 0.2–3	$(1 - 2800) \times 10^b$	2017
Italy	FERMI-FEL1	NC	1.5	0.01–0.06	10–50	2012
	FERMI-FEL2			0.06–0.3		2014
Japan	SACLA	NC	8	4–15	30–60	2011
Korea	PAL-XFEL	NC	10	1–20	60	2016
			3	0.3–1		
Switzerland	SwissFEL	NC	5.8	2–12	100	2017
			3	0.2–2		
USA	LCLS	NC	16	0.25–11	120	2009
	LCLS-II	NC	16	1–25	120	2020
	LCLS-II	SC	4	0.2–5	10^6	2020

^aPulsed mode operation at 10 Hz, with each macropulse providing up to 500 bunches.

^bPulsed mode operation at 10 Hz, with each macropulse providing up to 2800 bunches.





UCLA

Linac Coherent Light Source: The first five years

Christoph Bostedt,^{*} Sébastien Boutet, David M. Fritz, Zhirong Huang,
 Hae Ja Lee, Henrik T. Lemke,[†] Aymeric Robert, William F. Schlotter,
 Joshua J. Turner, and Garth J. Williams[‡]

*SLAC National Accelerator Laboratory, 2575 Sand Hill Road, Menlo Park,
 California 94025, USA*

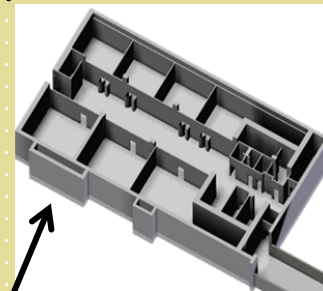
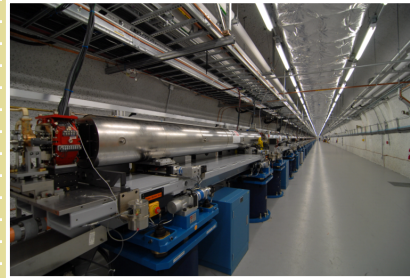
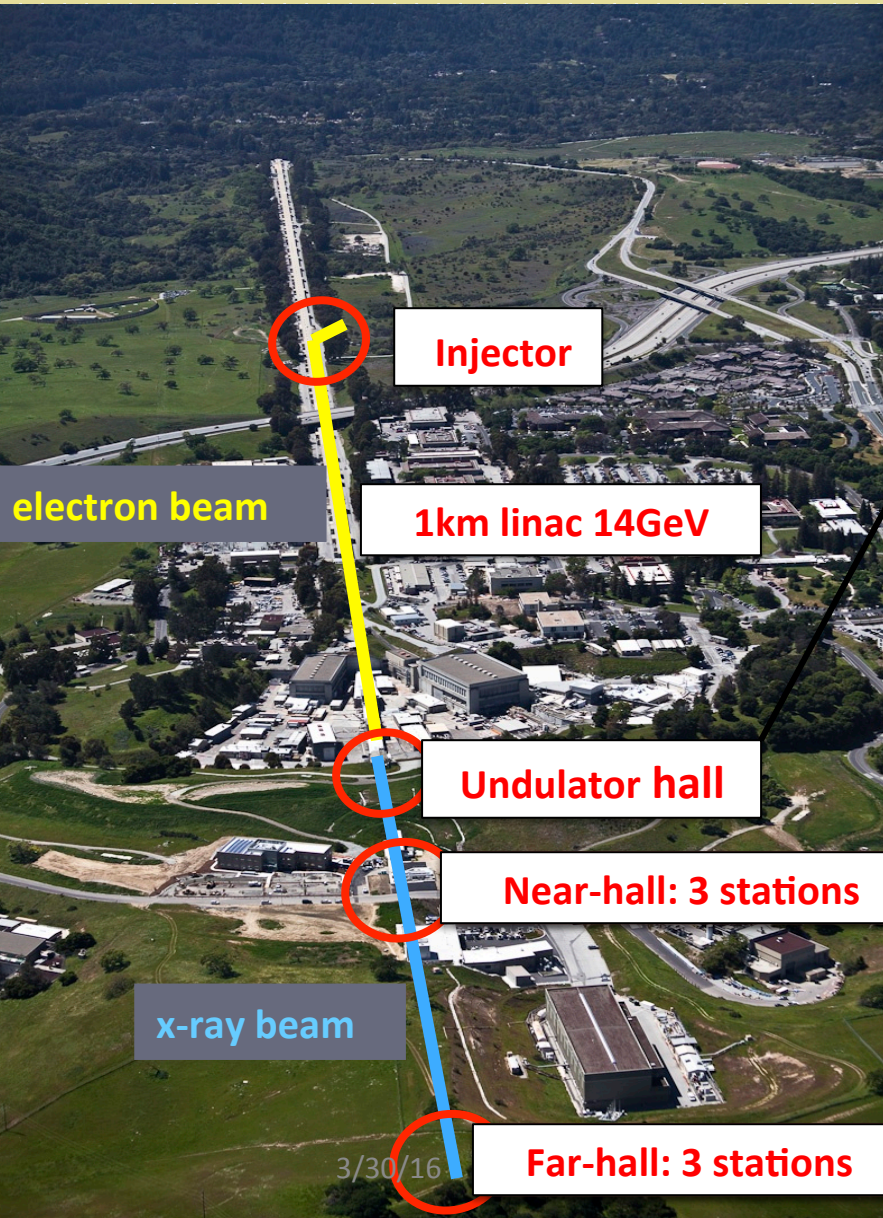
Parameter	Design	Typical	Unit
Photon energy range	800–8000	270–11 200	eV
Peak x-ray power	10	Up to 100	GW
X-ray pulse energy	2	2–4	mJ
Pulse repetition rate	120	120	Hz
SXR ^a bandwidth (FWHM)	0.1	0.2–2	%
SXR pulse duration (FWHM)	200	50–500	fs
SXR pulse energy jitter (rms)	20	3–10	%
SXR wavelength jitter (rms)	0.2	0.15	%
HXR ^b bandwidth (FWHM)	0.1	0.2–0.5	%
HXR pulse duration (FWHM)	200	30–100	fs
HXR pulse energy jitter (rms)	20	5–12	%
HXR wavelength jitter (rms)	0.2	0.05	%

Design and typical measured LCLS x-ray beam characteristics for soft x-ray (SXR) and hard x-ray (HXR) photon energies.

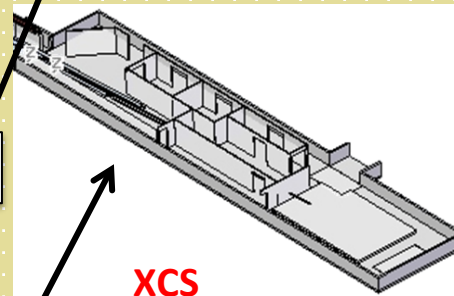
^aTypical soft x-ray photon energy is 830 eV.

^bTypical hard x-ray photon energy is 8.5 keV.

LCLS: the world's first x-ray free electron laser



AMO SXR XPP

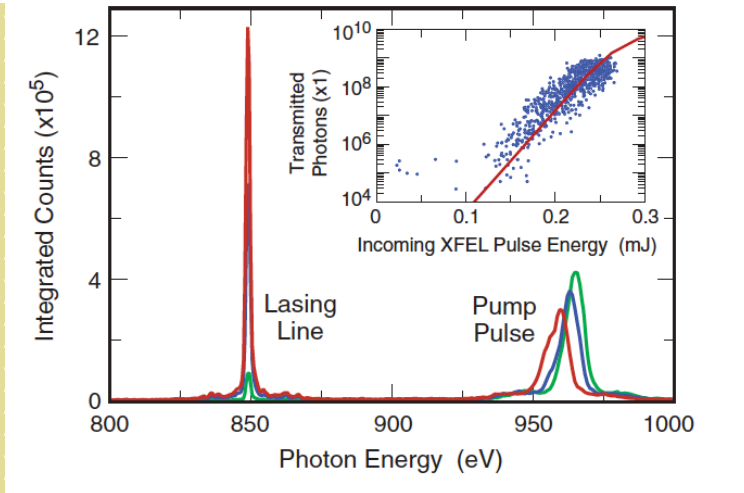
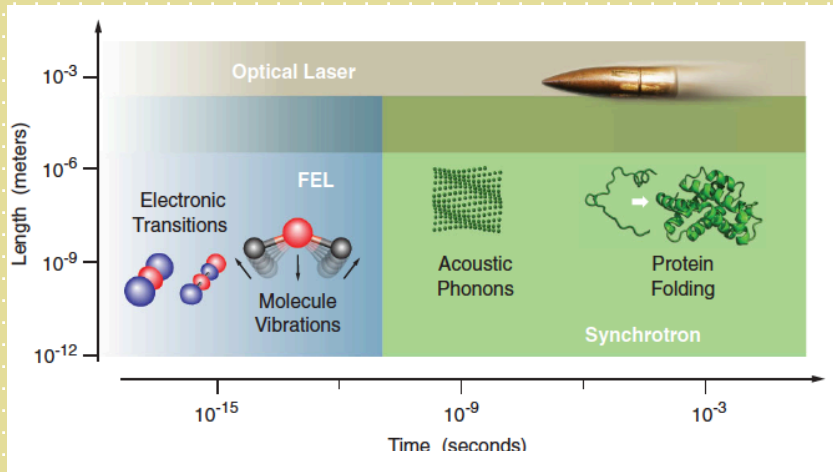
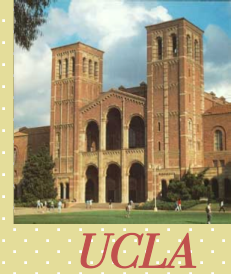


XCS
CXI
MEC

- [AMO: Atomic, Molecular & Optical Science](#)
- [CXI: Coherent X-ray Imaging](#)
- [MEC: Matter in Extreme Conditions](#)
- [SXR: Soft X-ray Materials Science](#)
- [XCS: X-ray Correlation Spectroscopy](#)
- [XPP: X-ray Pump Probe](#)

More instruments will be added with LCLS II, starting about 2018.

Atomic Molecular Optical Physics



X-ray pumped x-ray lasing. Selected single-shot spectra of the neon x-ray lasing line at 850 eV and simultaneously transmitted FEL pulse around 960 eV. The x-ray lasing line width is much narrower and jitter free. Rohringer, N., et al. 2012, Nature 481, 488.





Anomalous nonlinear X-ray Compton scattering

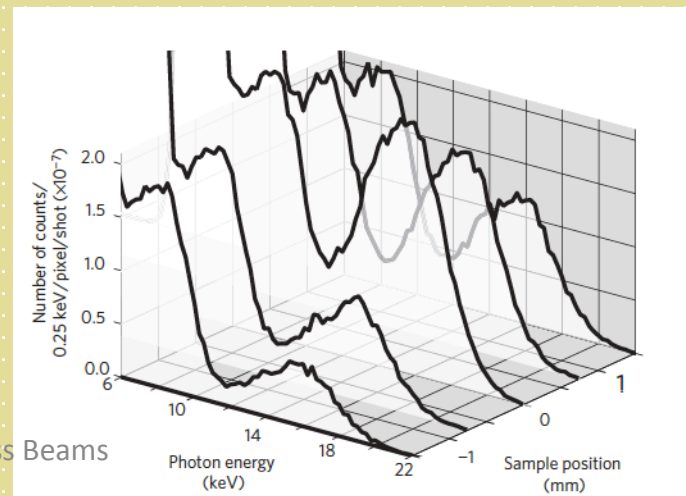
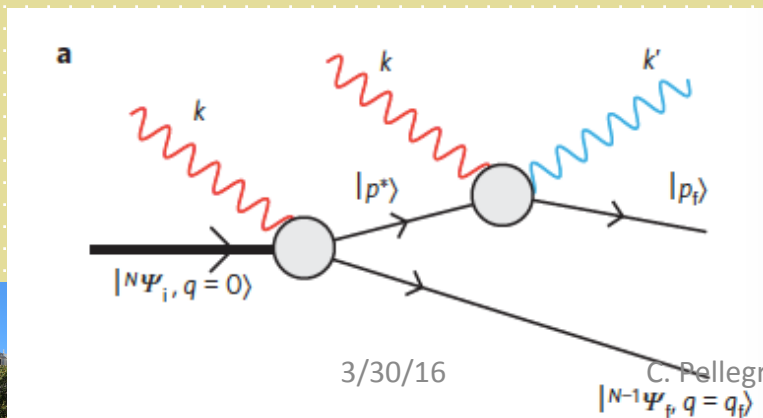
Matthias Fuchs et al.

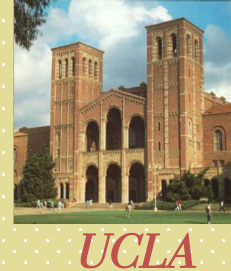
PUBLISHED ONLINE: 31 AUGUST 2015 | DOI: 10.1038/NPHYS3452

we report the observation of one of the most fundamental nonlinear X-ray–matter interactions: the concerted nonlinear Compton scattering of two identical hard X-ray photons producing a single higher-energy photon.

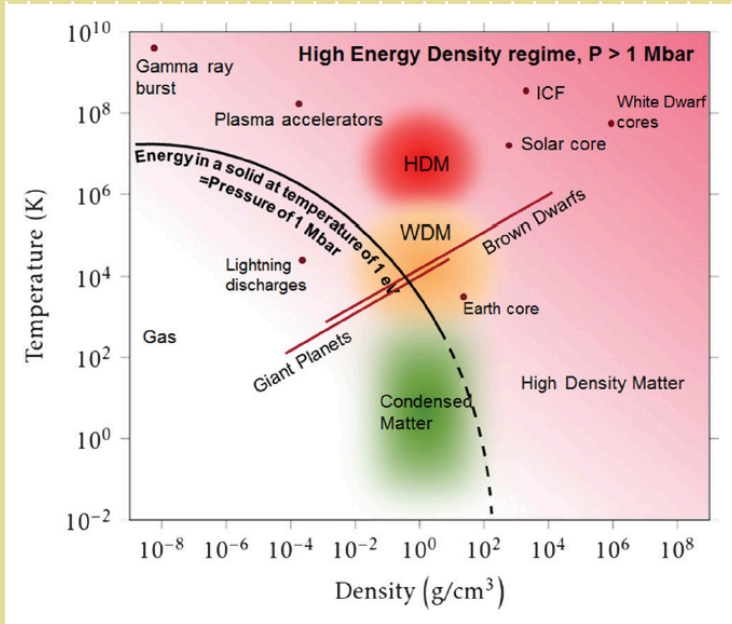
X-ray intensity reached $4 \times 10^{20} \text{ W/cm}^2$, corresponding to an electric field, $5 \times 10^{11} \text{ V/m}$, well above the atomic unit of strength and within almost four orders of magnitude of the quantum electrodynamics Schwinger critical field $\sim 10^{18} \text{ V/m}$

Incoming photon energy $\sim 9 \text{ keV}$, focus 100 nm, 1.5 mJ/pulse, 50 fs pulse duration.



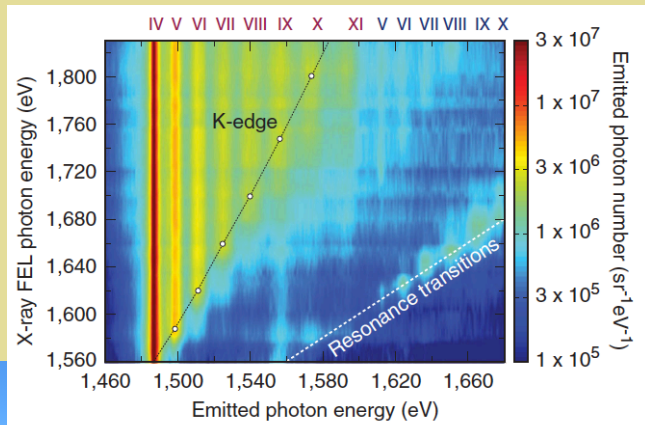


Warm dense matter, hot dense matter



Multiple experiments have used LCLS to irradiate a solid density sample and measure subsequent K-shell emission of dense aluminum plasmas, revealing saturation of the absorption induced by the ionization in the x-ray regime (Rackstraw et al., 2015) and much larger lowering of the ionization potential (Cho et al., 2012; Ciricosta et al., 2012; Vinko et al., 2012, 2015; Vinko, Ciricosta, and Wark, 2014) than predicted by commonly used plasma models (Stewart and Pyatt, 1966).

Vinko, S. M., et al., 2012, Nature (London) 482, 59.
 Vinko, S. M., et al., 2015, Nat. Commun. 6, 6397

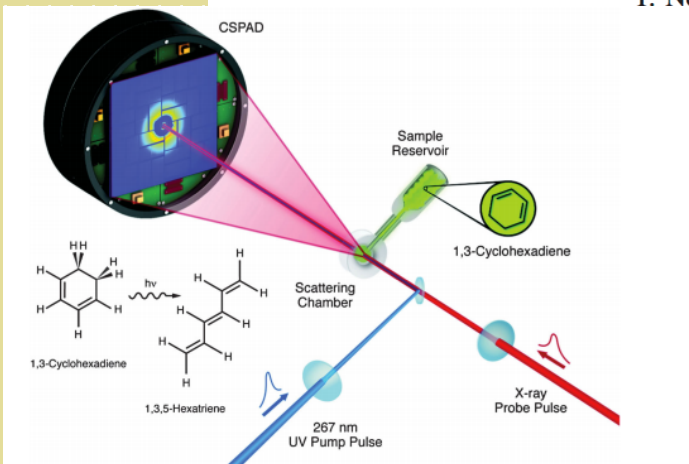




UCLA

Imaging Molecular Motion: Femtosecond X-Ray Scattering of an Electrocyclic Chemical Reaction

M. P. Minitti,^{1,*} J. M. Budarz,^{1,2} A. Kirrander,³ J. S. Robinson,¹ D. Ratner,¹ T. J. Lane,^{1,4} D. Zhu,¹ J. M. Glowia,¹ M. Kozina,¹ H. T. Lemke,¹ M. Sikorski,¹ Y. Feng,¹ S. Nelson,¹ K. Saita,³ B. Stankus,² T. Northey,³ J. B. Hastings,^{1,†} and P. M. Weber^{2,‡}



... .. By mapping nuclear motions using femtosecond x-ray pulses, we have created real-space representations of the evolving dynamics during a well-known chemical reaction and show a series of time- sorted structural snapshots produced by ultrafast time-resolved hard x-ray scattering.

Our analysis shows that, upon absorption of the optical photon, the chemical reaction of 1,3-cyclohexadiene to 1,3,5-hexatriene starts with a rapid expansion of the carbon bonds of the cyclohexadiene ring. ...

Within one or two oscillations of the carbon skeleton, the C1–C6 chemical bond breaks as the terminal carbon atoms move perpendicular to the molecular plane along the reaction coordinate. It is already at this point that the terminal hydrogen atoms of the nascent hexatriene molecule align to conform to the Woodward-Hoffman rules [16]. Consequently, the stereochemical fate of the chemical reaction is sealed as early as 30 fs after the optical excitation.





X-ray FELs impact on structural biology

510

Biophysical Journal Volume 106 February 2014 510–525

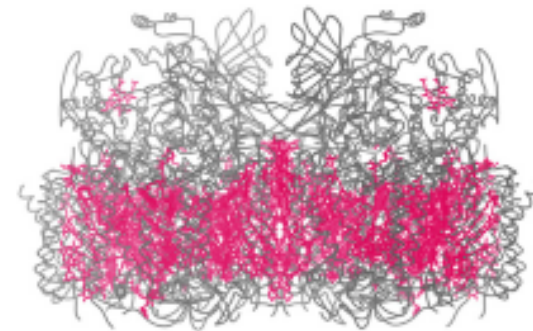
Biophysical Highlights from 54 Years of Macromolecular Crystallography

Jane S. Richardson* and David C. Richardson
 Biochemistry Department, Duke University, Durham, North Carolina

ABSTRACT The United Nations has declared 2014 the International Year of Crystallography, and in commemoration, this review features a selection of 54 notable macromolecular crystal structures that have illuminated the field of biophysics in the 54 years since the first excitement of the myoglobin and hemoglobin structures in 1960. Chronological by publication of the earliest solved structure, each illustrated entry briefly describes key concepts or methods new at the time and key later work leveraged by knowledge of the three-dimensional atomic structure.

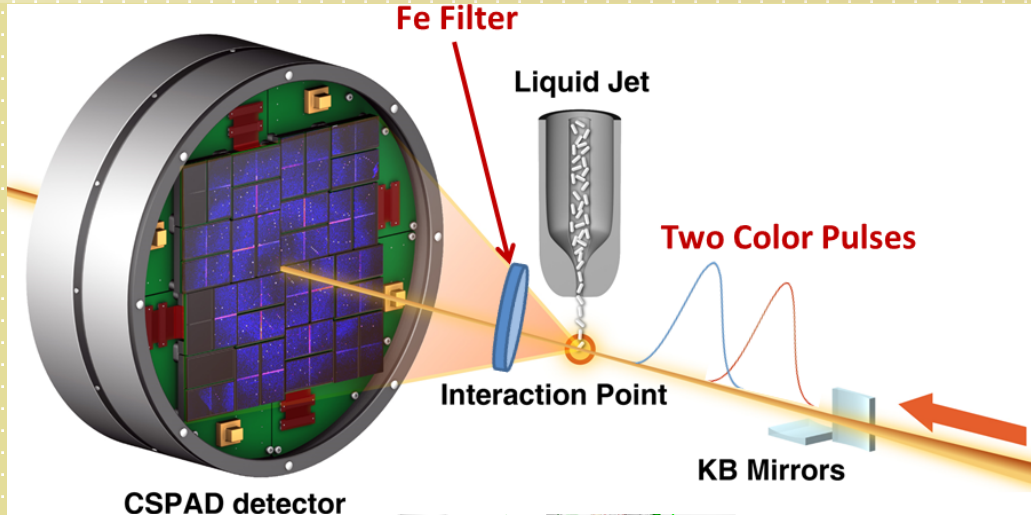
54. Free-electron laser crystallography

Free-electron laser crystallography is without question the most spectacular new technical development in the field. A jet of droplets with nanocrystals is sent past a beam of femtosecond x-ray laser pulses, and diffraction is recorded before the crystal has time to explode. This has the potential for determining otherwise intractable molecular structures and for accessing rapid time steps. The many challenging problems with data and analysis appear to be solvable. After demonstration structures of photosystems and lysozyme (e.g., PDB:3PCQ (126), PDB:4FBY (127), PDB:4ET8 (10)), there is now a novel structure of propeptide-inhibited trypanosomal cathepsin B (PDB:4HWY (128)) potentially useful for drug design. (Fig. 54. $C\alpha$ splines and chromophores (pink) in Photosystem II (PDB:4FBY)).

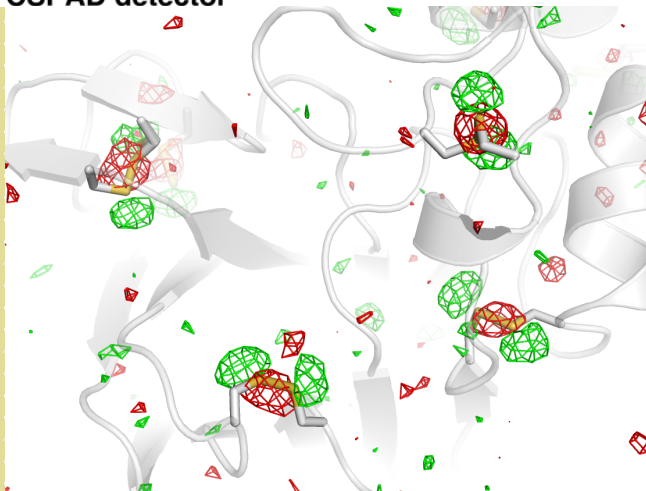


Imaging Molecular Damage at the fs Time-Scale

Courtesy of S. Boutet



High-Energy pump absorbed by filter.
 Low-energy probe goes through.
 Use short pulses (~10-15 fs)
 Vary delay and look at difference electron density maps.



Thaumatin Molecule

Difference between unperturbed sample and pump-probe (100 fs delay).

Green: positive electron density
Red: negative electron density

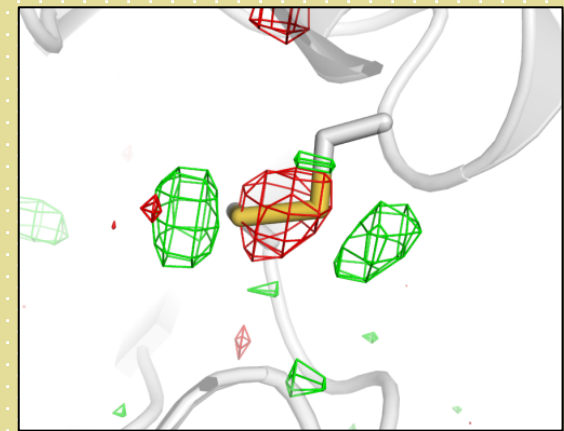
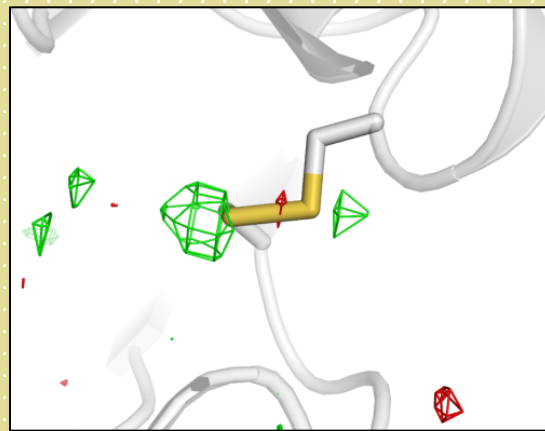
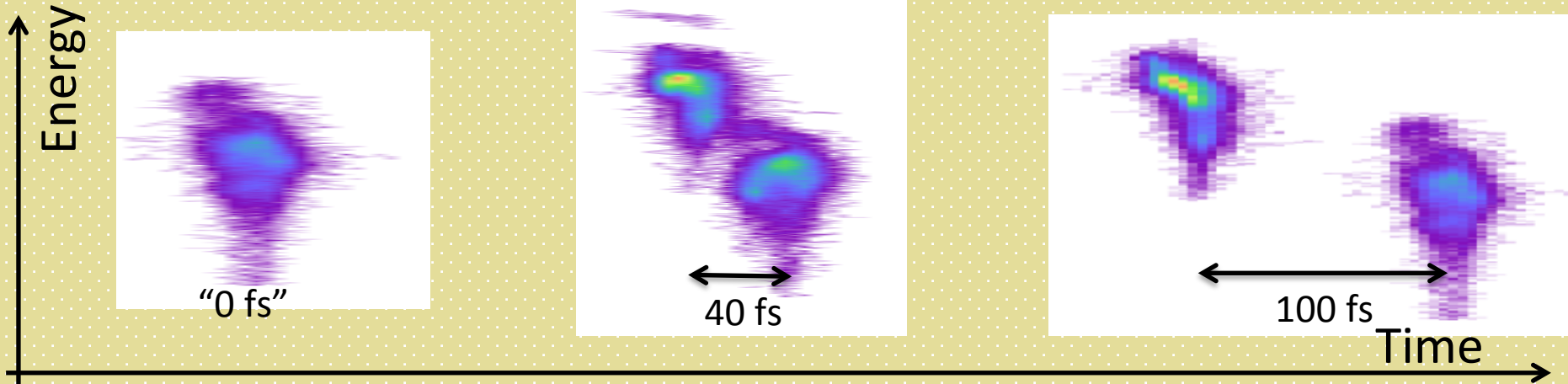


Movie of Molecular Explosion

Courtesy S. Boutet



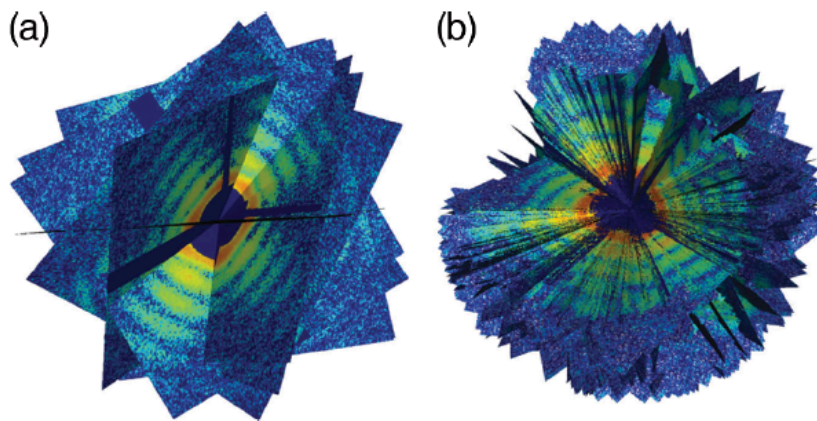
Vary time-delay to make a "movie" of the process.



Single Particle Imaging

X-ray FELs such as LCLS can in principle provide a path to single-particle imaging (SPI) by collecting 2D coherent diffractive imaging patterns from individual noncrystalline particles and assembling a three-dimensional pattern from multiple copies of sufficiently identical particles. The promise of single-particle imaging is tantalizing, with all the challenges related to crystal growth and crystallography in general removed. Studying single molecules free of the crystal contacts and interactions that may distort their structure at room temperature would be revolutionary. The extremely weak signal, especially at high resolution, expected from single biological molecules makes imaging them in this way very challenging.

Assembled three-dimensional mimivirus diffraction pattern from 198 2D diffraction patterns. (a) Subset of ten diffraction patterns shown in their best orientation. (b) All 198 diffraction patterns shown with a cutout showing the origin in reciprocal space. Adapted from Ekeberg, T., et al., 2015, Phys. Rev. Lett. 114, 098102.

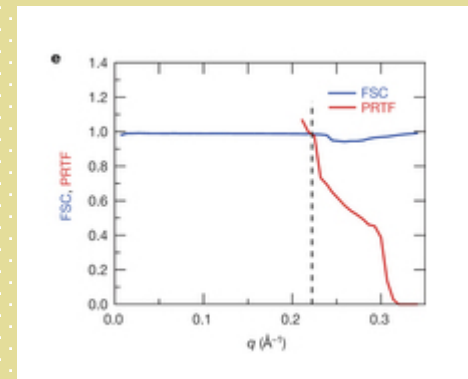
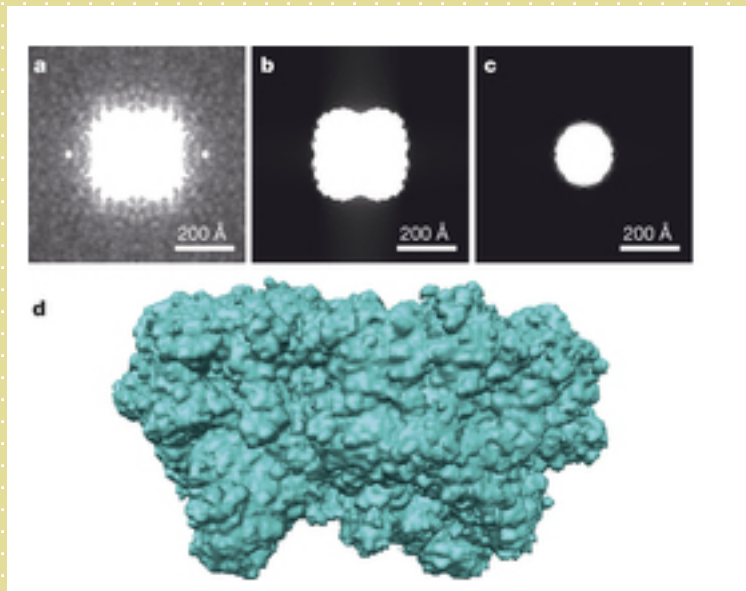




One important step toward single molecule imaging.

Macromolecular diffractive imaging using imperfect crystals

H. Chapman et al. Nature, 2016, 530, 202-206



Obtained by combining analysis of the Bragg peaks and of the continuous diffraction (oversampling) yielding the autocorrelation function

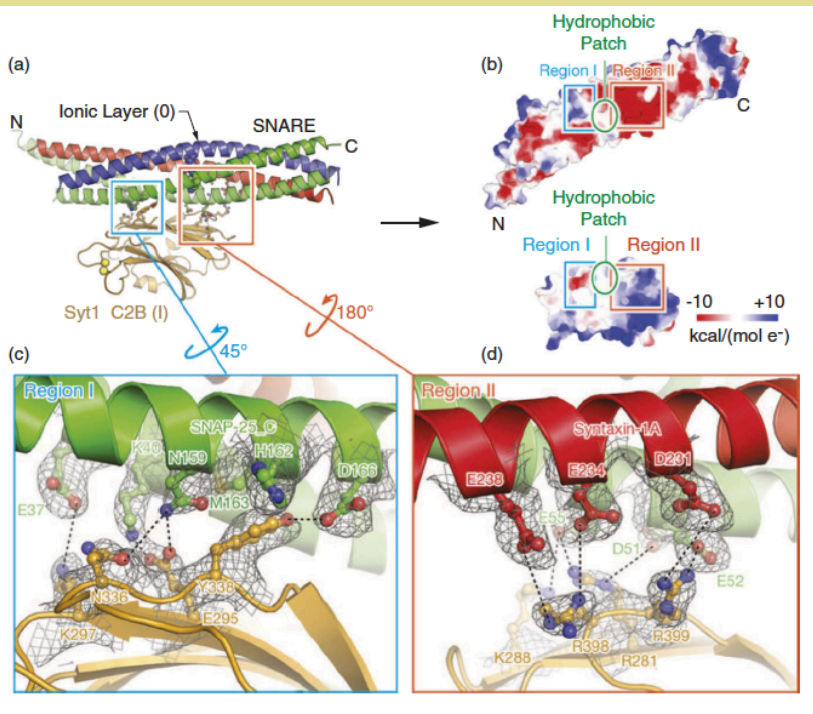


Neuroscience



The interaction between synaptotagmin-1 and the neuronal SNARE (soluble n-ethylmaleimide sensitive factor attachment protein receptor) complex was studied at a resolution of 3.5 Å (Zhou et al., 2015). This interaction is critical in neurotransmitter release.

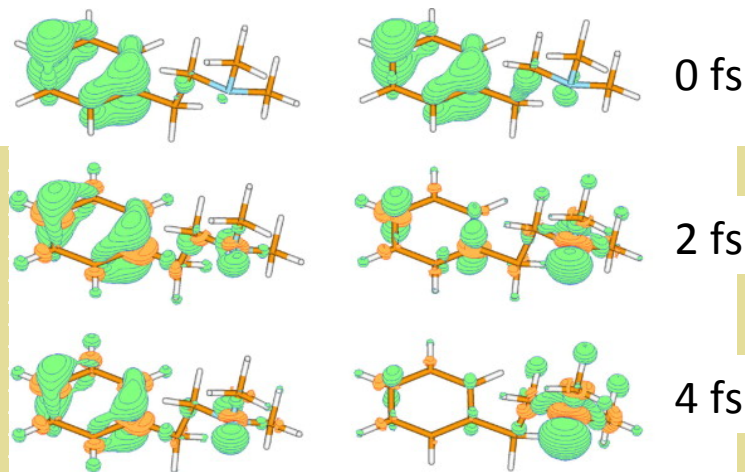
Interface between synaptotagmin and the neuronal SNARE complex. (a) The primary interface along with interacting residues. (b) Electrostatic potential map of the primary interface shows how two polar regions I and II are connected by a hydrophobic patch (SNAP-25 I44, L47, and V48 and Syt1 V292, L294, and A402). (c), (d) Close-up views of regions I and II. Labels indicate interacting residues. Dashed lines indicate hydrogen bonds or salt bridges. 2 mF_o DF_c electron density maps of the interacting residues are superimposed (gray mesh; contour level . 1.5σ). Adapted from Zhou, Q., et al., 2015, Nature



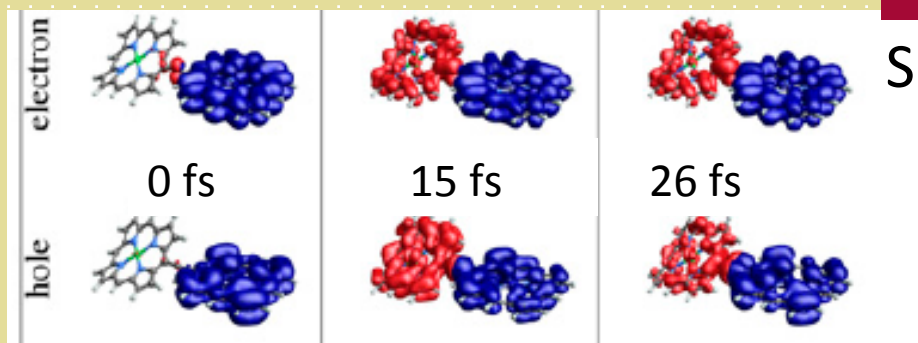
Motivation for SXR sub-fs pulses

...many of our great challenges in energy science, materials science, and bioscience require new insights that lie beyond this femtosecond barrier

1) Charge migration
(example: 2-phenylethyl-N-N-dimethylamine)



2) Stimulated X-ray Raman Redistribution:
(example: Metalloporphyn)



3) Damage-free experiments

From:

NEW SCIENCE OPPORTUNITIES
ENABLED BY LCLS-II X-RAY LASERS

June 1, 2015

SLAC-R-1053



X-ray FELs: Present Status



UCLA

Four X-ray FELs are in operation: LCLS at SLAC, SACLA in Japan, FLASH in Germany, Fermi in Italy, covering the wavelength range from 0.6 Å to 100 nm .

Swiss FEL, Korean FEL, European XFEL, LCLS-II are under construction and will start operation in the next two to three years.

General characteristics of X-ray pulses can be summarized as follows:

- Pulse energy hundreds of μJ to few mJ;
- Good transverse coherence
- Line width about 10^{-3} to 10^{-4}
- Pulse duration from a few to about 100 fs;
- About 2×10^{12} photons/pulse at 1 Å, 100 fs, more at longer wavelengths.
- Pulse repetition rate from about 100 Hz to 10^5 to 10^6 for LCLS-II.



The physics of x-ray free-electron lasers

C. Pellegrini

*Department of Physics and Astronomy, University of California at Los Angeles,
Los Angeles, California 90095, USA
and SLAC National Accelerator Laboratory, Menlo Park, California 94025, USA*

A. Marinelli

SLAC National Accelerator Laboratory, Menlo Park, California 94025, USA

S. Reiche

Paul Scherrer Institute, 5232 Villigen PSI, Switzerland



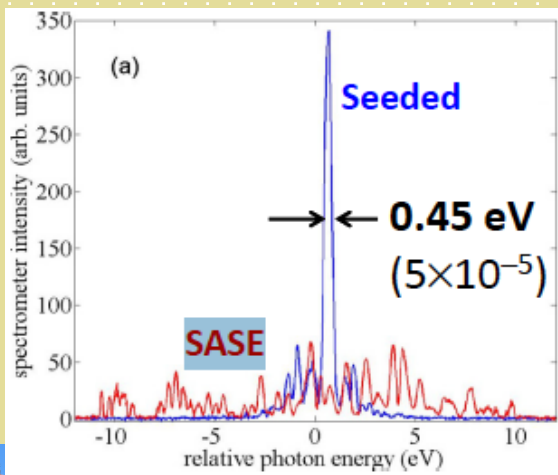
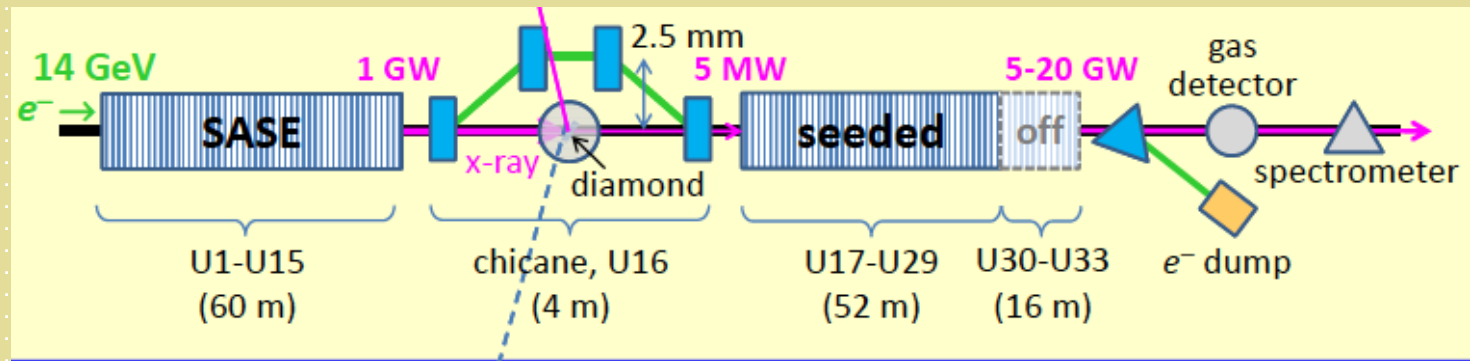
UCLA



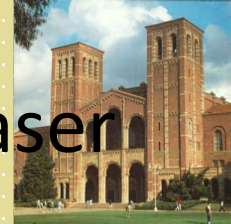


Improving LCLS temporal coherence: Self-seeded spectra

Self-seeding is a way to improve the spectrum and reduce the line-width using the transmission around the stop band of a Bragg reflection in a diamond crystal, Geloni, G., V. Kocharyan and E. Saldin, 2011, Journal of Modern Optics **58**, 16.

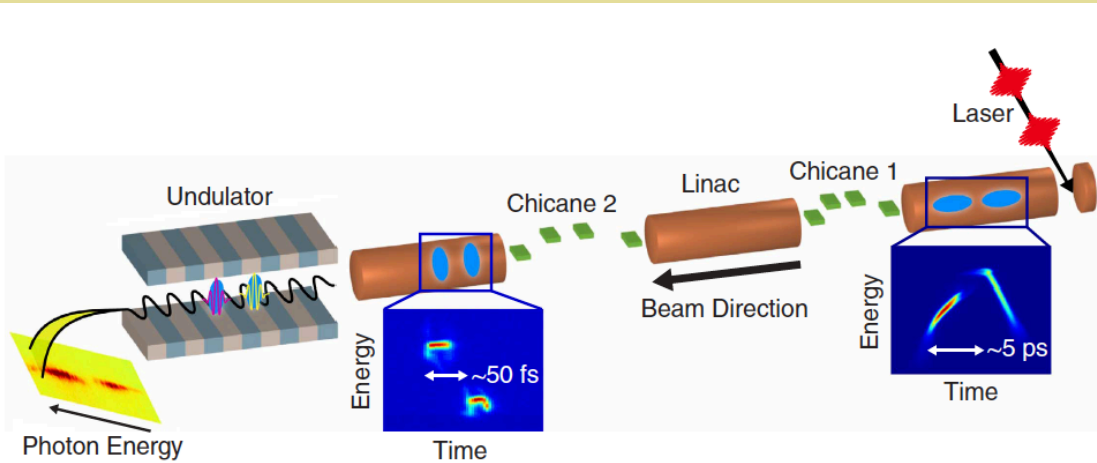


The concept as been demonstrated at LCLS , J. Amann, et al. Nature Photonics, DOI: 10.1038/NPHOTON 2012.180

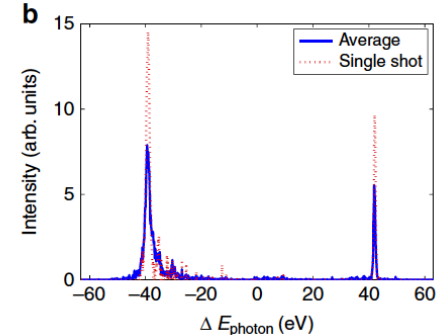
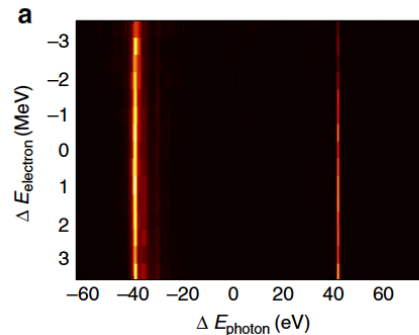
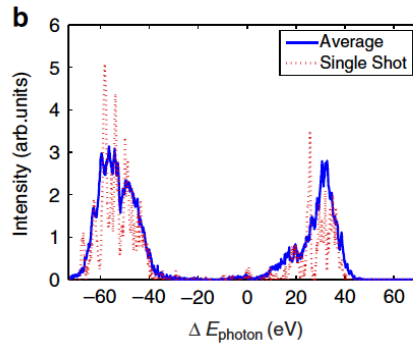
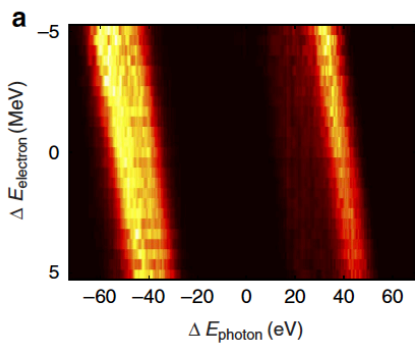


High-intensity double-pulse X-ray free-electron laser

A. Marinelli¹, et al., Nature Comm., DOI: 10.1038/ncomms7369



Double laser pulse on cathode generates two electron bunches separated in time, 0-100 fs, and energy, ~100eV. Average photon energy 8.3keV. Used in pump-probe experiments.

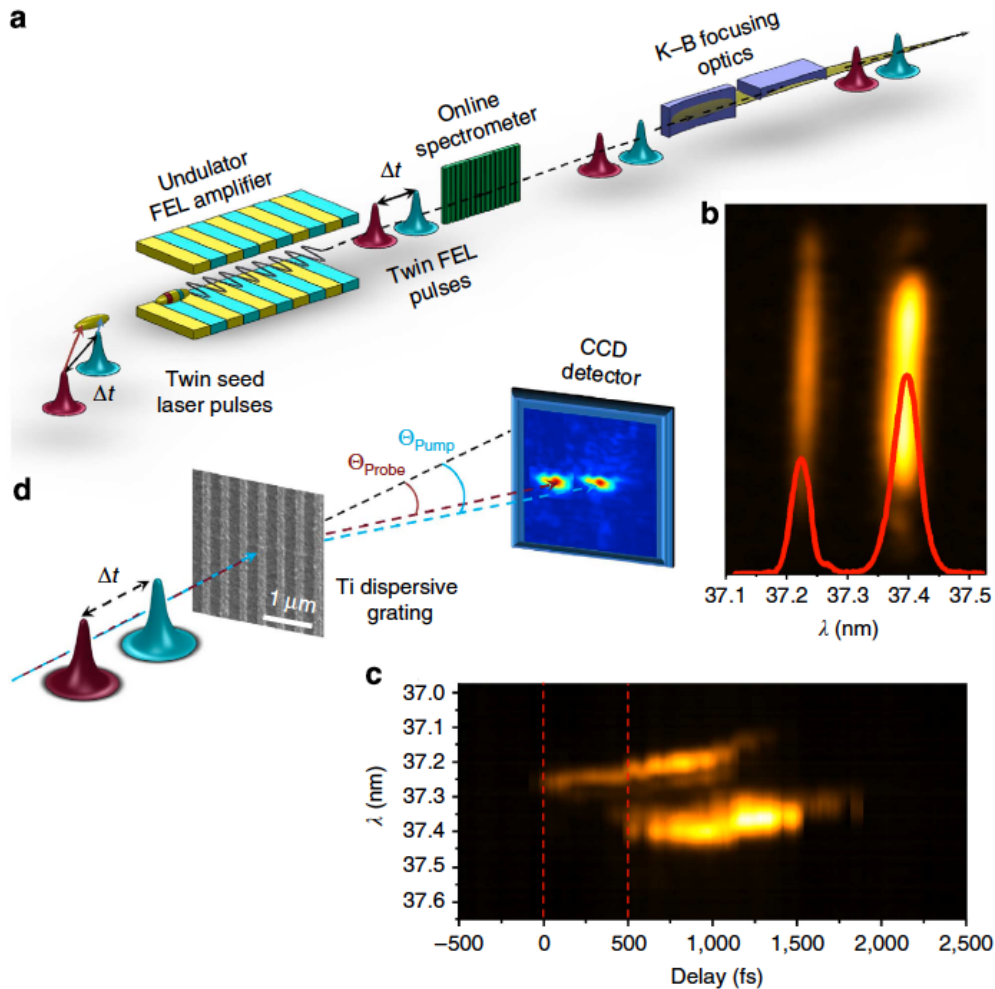


Spectral measurements: SASE, left; self-seeding, right. (a) Intensity as a function of beam energy and photon energy (b) Average and single-shot for fixed beam energy.



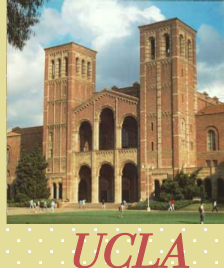


Two-color pump-probe experiments with a twin pulse seed extreme ultraviolet free-electron laser, E. Allaria et al. Nature Comm., DOI: 10.1038/ncomms3476 (2013)



Fermi uses two different wavelength seed laser pulses, 180 fs long, seed at 260-262 lambda, fundamental at 784 nm, color separation inside gain bandwidth. The two pulses are separated in time and in wavelength.





PRL 110, 134801 (2013)

PHYSICAL REVIEW LETTERS

week ending
29 MARCH 2013

Experimental Demonstration of Femtosecond Two-Color X-Ray Free-Electron Lasers

A. A. Lutman, R. Coffee, Y. Ding,^{*} Z. Huang, J. Krzywinski, T. Maxwell, M. Messerschmidt, and H.-D. Nuhn

Demonstration Of Two-color X-FEL Operation and Autocorrelation Measurement at SACLA, T.Hara, Y. Inubushi, T. Ishikawa, H. Tanaka, T. Tanaka, K. Togawa, M. Yabashi, T. Katayama, T. Togashi, K. Tono, T. Sato, Proc. of the 2013 FEL Conf. New York

PRL 111, 134801 (2013)

PHYSICAL REVIEW LETTERS

week ending
27 SEPTEMBER 2013

Multicolor Operation and Spectral Control in a Gain-Modulated X-Ray Free-Electron Laser

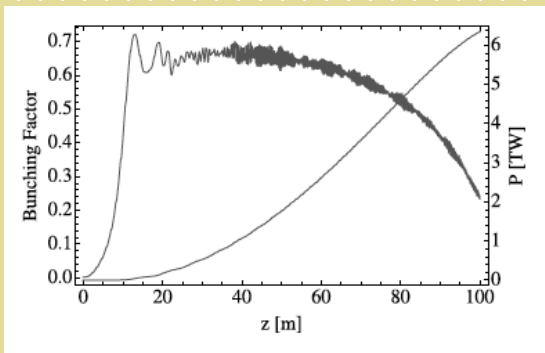
A. Marinelli,^{1,*} A. A. Lutman,¹ J. Wu,¹ Y. Ding,¹ J. Krzywinski,¹ H.-D. Nuhn,¹ Y. Feng,¹ R. N. Coffee,¹ and C. Pellegrini^{2,1}



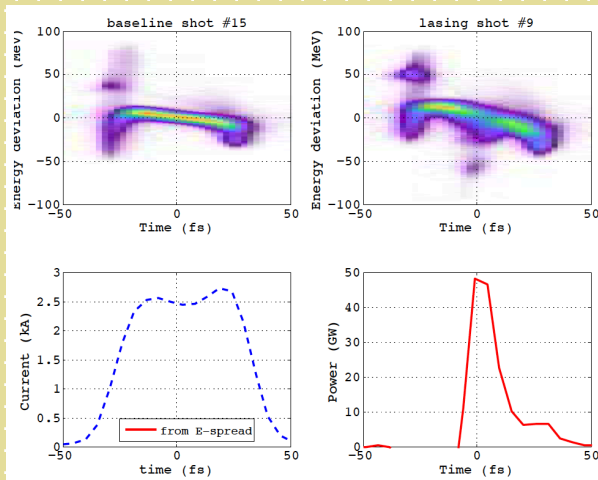
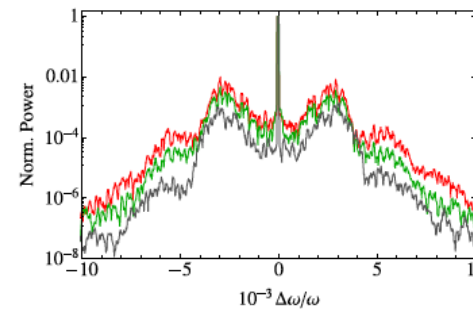


High efficiency, multiterawatt x-ray free electron lasers

C. Emma,¹ K. Fang,² J. Wu,² and C. Pellegrini^{1,2}



5 MW Not Optimized
5 MW Optimized
25 MW Optimized





Future developments

1. TW peak power to enable SPI, nonlinear science, multiple beam lines from one undulator.
2. Attosecond pulses
3. Multicolor spectra
4. More photons/fs/ $(\Delta\omega/\omega)$
5. Pump probe from the same electron bunch





Note on TW X-ray FELs

To reach the multi TW level we need:

1. Tapering with large seeding signal to minimize sideband instability effects.
2. Minimize the gain length->Maximize the FEL parameter->Maximize beam plasma frequency $\rho \propto I_{peak} / \beta\epsilon$
3. We need a specialized undulator design, short undulator section, order gain length, strong, distributed focusing.





Conclusions

To increase the scientific area that X-ray FELs can explore we should concentrate research and development on:

1. Advanced, strong focusing undulators for TW peak power, multiple beam lines
2. Attosecond pulses in a pump-probe configuration
3. Improved and flexible spectral properties, including multicolor pulses

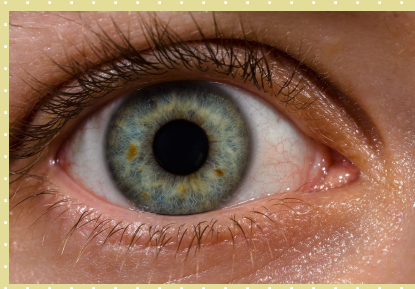
To make X-ray FRLs more compact, less expensive:

1. Advanced e-gun, improved brightness
2. More compact accelerators
3. Improved instrumentation





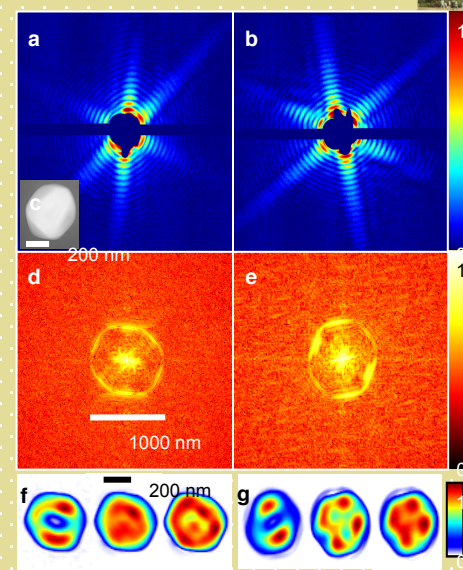
Conclusions: 390 years of exploration of the microscopic world



Resolution: ~0.1 mm, 0.1 sec



LCLS, 2009



Imaging single mimivirus
Seibert et al,
Nature, 470, 78 (2011)

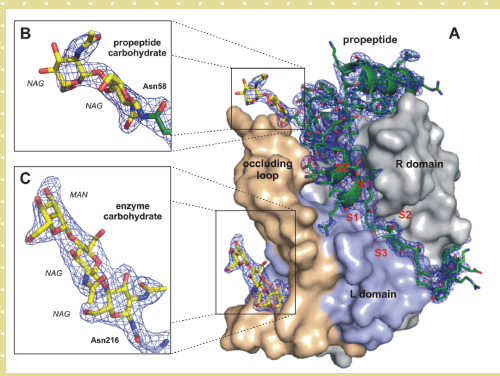
Accademia da Lincei: "Microscopium"



Francesco Stelluti
1577- ca 1651

F. Stelluti, 1625
Galileian microscope

Resolution: ~0.01 mm, 0.1 sec



Natively Inhibited
Trypanosoma brucei
Cathepsin B Structure
Determined by Using an X-
ray Laser, L. Redecke et al.
Science 339, 227 (2013)

Resolution: ~few Å,
few fs